Journal of Composite Materials

http://jcm.sagepub.com

Structural Integrity of Composite Columns Subject to Fire

George A. Kardomateas, George J. Simitses and Victor Birman

Journal of Composite Materials 2009; 43; 1015 originally published online Feb 24, 2009;
DOI: 10.1177/0021998308097733

The online version of this article can be found at:
http://jcm.sagepub.com/cgi/content/abstract/43/9/1015

Published by:

http://www.sagepublications.com

On behalf of:

American Society for Composites

Structural Integrity of Composite Columns Subject to Fire

GEORGE A. KARDOMATEAS AND GEORGE J. SIMITSES
School of Aerospace Engineering, Georgia Institute of Technology
Atlanta, Georgia 30332-0150, USA

VICTOR BIRMAN*
Engineering Education Center, Missouri University of Science and Technology, (Formerly University of Missouri-Rolla)
One University Boulevard, St. Louis, Missouri 63121, USA

ABSTRACT: This article investigates the thermal response of an axially restrained composite column, which is exposed to a heat flux due to fire. The heat damage, the charred layer formation and nonuniform transient temperature distribution in the column exposed to fire from one side are calculated by the thermal model developed by Gibson et al. [1]. For the thermal response analysis, the mechanical properties of the fire-damaged (charred) region are considered negligible, while the degradation of the elastic properties with temperature in the undamaged layer (especially near the glass transition temperature of the matrix) is accounted for using experimental data for the elastic moduli. Due to the nonuniform stiffness distribution through the thickness and the effect of the ensuing thermal moment, the structure behaves like an imperfect column, and responds by bending rather than buckling in the classical Euler (bifurcation) sense. Another important effect of the non-uniform temperature is that the neutral axis moves away from the centroid of the cross-section, resulting in an additional moment due to eccentric mechanical loading, which tends to bend the structure. The compressive behavior of a column subjected to simultaneous high intensity surface heating and axial compressive loading was investigated experimentally to verify the anticipated theoretical response. All specimens exhibited bending and subsequent catastrophic failure, even at compressive stresses well below these corresponding to the Euler load.

KEY WORDS: composite column, fire, thermal response, bending.

INTRODUCTION

FIBER REINFORCED POLYMERIC composites are used extensively in aerospace, marine, infrastructure and chemical processing applications. In all these applications, fire

*Author to whom correspondence should be addressed. E-mail: vbirman@mst.edu
Figure 4 appears in color online: http://jcm.sagepub.com

0021-9983/09/09 1015–19 $10.00/0 DOI: 10.1177/0021998308097733

events and the resulting effects on the structural integrity are of considerable concern. In addition to the implications for design, quantitative information regarding the nature of the strength loss is required to make decisions regarding, for example, the seaworthiness of a ship that has sustained fire damage.

Many of the thermal properties of composites related to fire have been thoroughly studied and are well understood, including ignition times, heat release rates, smoke production rates and gas emissions (e.g., Sorathia et al. [2], Gibson and Hume [3]). Also, recent work on the post-fire residual properties (Mouritz and Gardiner [4]) showed large reductions to the edgewise compression capacity of phenolic-based sandwich composites despite their good flame resistance. However, an important gap that remains in the understanding of composites is their response and structural integrity due to the combined effect of mechanical and thermal loading due to fire. The present article addresses this issue on the example of a symmetrically laminated composite column. It is illustrated that such column that would experience bifurcation buckling as a result of compressive loading exhibits bending in the presence of fire. The article expands the previous analysis [5] providing detailed explanations of the solution methodologies for different boundary conditions and nonlinear and linear formulations. The equivalent linearization approach described in the article can be applied to generate accurate approximate solutions. Contrary to the previous study [5] that concentrated on the effect of the heat flux on the response, this article emphasizes the time-dependent nature of the behavior of the column. In particular, the results are shown for the changes in the thickness of the charred layer, the thermally-induced bending moment, axial constraint stress and deflections as functions of the exposure time.

The column analyzed in this article is shown in Figure 1. This figure reflects the presence of a charred layer on the side of the column directly affected by fire. The length and total thickness of the column are denoted by L and H respectively. The thickness of the undamaged layer is represented by l, which is dependent on the time, t. Two cases shown in Figure 1 refer to different boundary conditions discussed below in the article.

ANALYSIS

Thermal Model for the Temperature and Char Distribution

The problem of predicting the behavior of polymer composite materials exposed to a fire environment may be divided into two different aspects, namely internal and external processes. The internal processes include all physical and chemical transformations which occur in the laminate. The external processes involve the determination of the shape, size and intensity of the flame in the boundary layer and, secondly, heat transfer from this frame to the affected laminate. The finite element model used in the article to predict the behavior of a GRP laminate subject to the fire environment is based on the mathematical model proposed by Henderson et al. [6] and further developed by Looyeh et al. [7] and Gibson et al. [8]. Following this approach, the non-linear partial differential equations that govern the behavior of the laminate in subject to fire are solved numerically using a mixed explicit-implicit finite element technique. Accordingly, the amount of the remaining resin material can be obtained as a function of the exposure time. Based on the experiments and calculations performed by Gibson et al. [8], we assume that when the residual resin context is less than 80%, the material can be treated as charred. A typical temperature distribution through the thickness of a composite column subject to fire is shown in Figure 2,

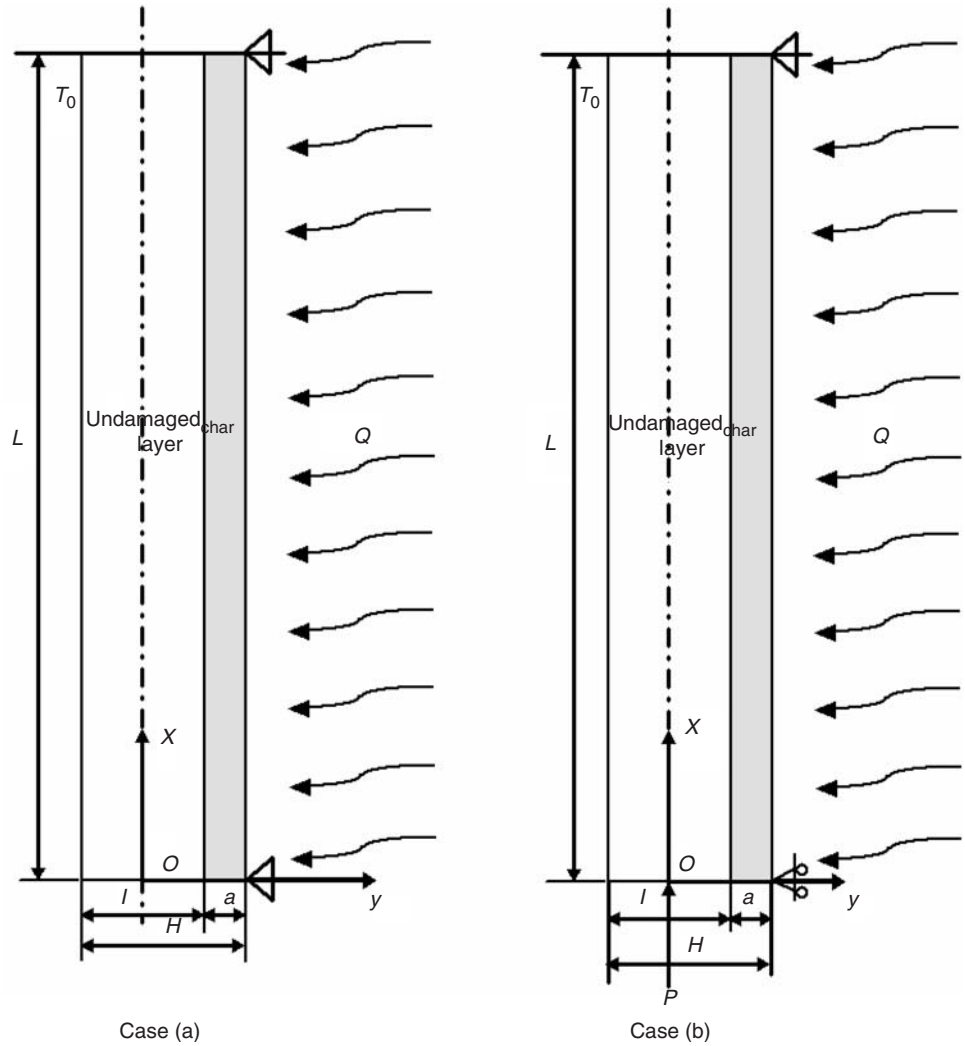

Figure 1. *Definition of the geometry for the laminated column, which is composed of an undamaged layer and a charred layer, and subjected to a combination of the heat flux due to fire, Q, and a compressive load, P. Case (a): immovable ends, case (b): axially unconstrained column.*

while the normalized thickness of a charred layer in the same column is depicted in Figure 3 (both figures are discussed in detail in the section on numerical results).

Thermomechanical Analysis: Formulation

The predicted temperature and charred layer thickness distribution with time along the thickness direction can be obtained by the thermal finite element model referred to in the previous section. The thermal buckling response of the column consisting of an undamaged layer and a charred layer, as shown in Figure 1, is analyzed by the quasi-static assumption. This assumption means that at each time instant the column is in an equilibrium state and

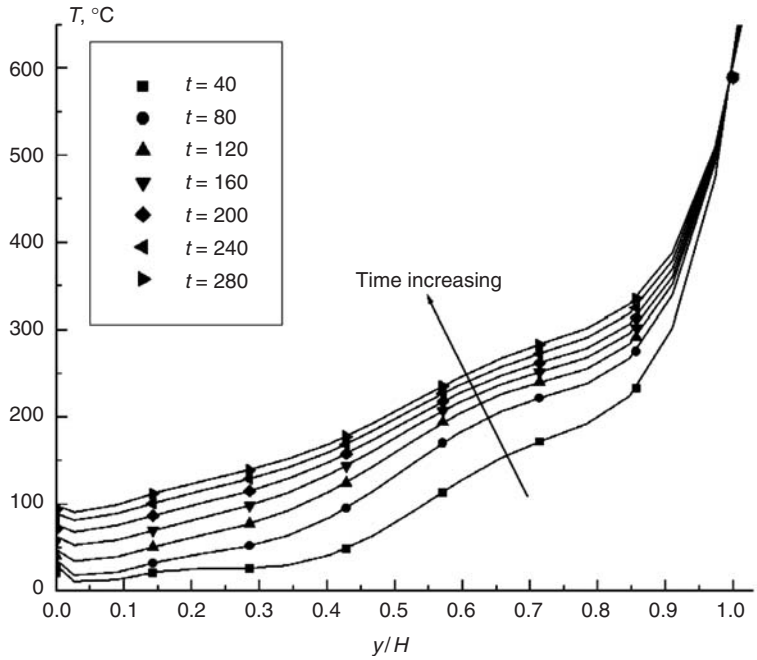

Figure 2. *Temperature distribution in the column subjected to heat flux $Q = 25\,kW/m^2$, the through-the-thickness y-coordinate is normalized with respect to the total thickness of the column. The seventh order polynomial fit curves are obtained by interpolation.*

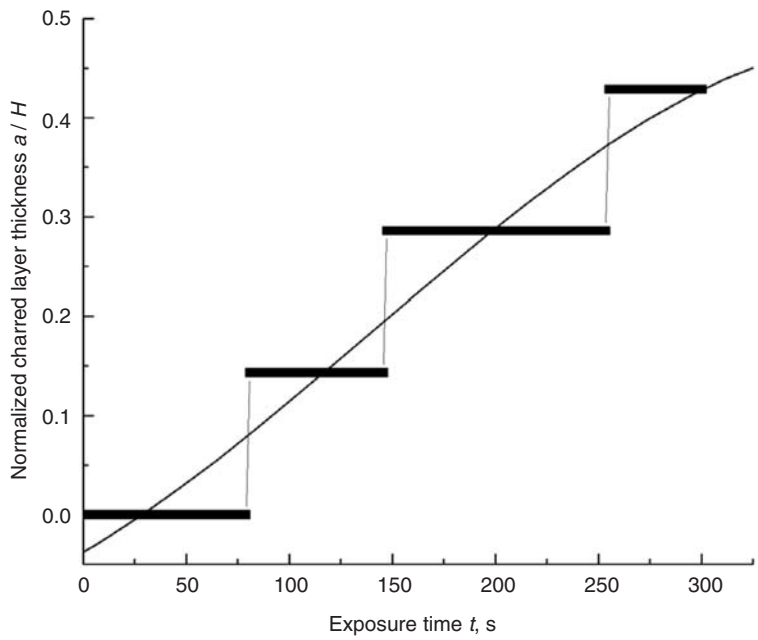

Figure 3. *Variation of the normalized thickness of the charred layer with the exposure time, which is not a continuous function, due to the assumption that the resin becomes fully charred when its residual content drops below 80%. The fire heat flux is $Q = 25\,kW/m^2$.*

the temperature distribution and the charred layer thickness obtained by the finite element model can be used in the static analysis. Such assumption is justified by a relatively long process of char formation as compared to the period corresponding to the fundamental frequency of a typical column. It is further reasonable to conservatively assume that the mechanical properties of the charred (fire-damaged) layer are negligible because of the thermal decomposition of resin material. Therefore, we only considered the undamaged layer in the thermomechanical response analysis, although the temperature distribution in the undamaged region has been obtained accounting for the existence of the char layer.

It is well known that the elastic modulus, E, of polymers depends strongly on the temperature, especially in the vicinity to the glass transition temperature, T_g, of the matrix. A recent paper by Kulcarni and Gibson [9] studied the effects of temperature on the elastic modulus of E-glass/vinyl-ester composites providing measurements of temperature dependence of the elastic modulus of the composite in the range of 20–140°C. The glass transition temperature of the matrix considered in Ref. [9] was $T_g = 130°\text{C}$. Near this temperature, the elastic modulus shows a significant variation in response to small temperature changes, but below T_g the variation is relatively small. As can be observed from Figure 4, the variation of the modulus reported in Ref. [8] can conveniently fit a third order polynomial equation. If E_0 denoted the modulus at room temperature, $T_0 = 20°\text{C}$, the modulus E can be represented as the following function of temperature T:

$$\begin{aligned}\frac{E}{E_0} &= 1 - a_1\left(\frac{T - T_0}{T_g - T_0}\right) + a_2\left(\frac{T - T_0}{T_g - T_0}\right)^2 - a_3\left(\frac{T - T_0}{T_g - T_0}\right)^3 \\ &= 1 - a_1\left(\frac{\Delta T}{\Delta T_g}\right) + a_2\left(\frac{\Delta T}{\Delta T_g}\right)^2 - a_3\left(\frac{\Delta T}{\Delta T_g}\right)^3\end{aligned} \tag{1}$$

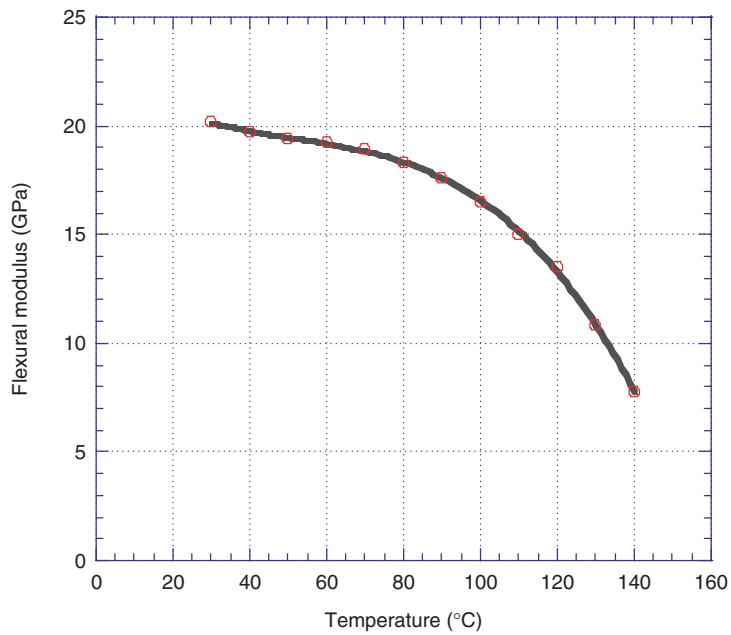

Figure 4. *The effects of temperature on the elastic modulus of pseudo-isotropic E-glass/vinyl-ester composites (based on data from [9]).*

where for the E-glass/vinyl-ester, $E_0 = 20.6$ GPa and $a_1 = 0.348$, $a_2 = 0.715$, and $a_3 = 0.843$. The composite studied in Ref. [9] has a fiber volume fraction of 0.516 and consists of five sub-layers with the orientation of each sub-layer [0/90/+45/−45/Random]. Accordingly, the modulus shown in Equation (1) can be interpreted as that for an equivalent pseudo-isotropic material. Equation (1) captures the physics of the non-linear dependence of the composite modulus on the glass transition temperature of the matrix, T_g. Temperature distribution in the undamaged layer, ΔT, that is present in Equation (1) can be determined from the finite element analysis, as described in the previous section.

In order to simplify the subsequent formulation for the thermomechanical response analysis, the axis x is located at the mid-surface of the undamaged layer, as shown in Figure 1. Now we define an 'average' modulus E_{av} and 'first' and 'second' moments of the modulus with respect to the mid-surface, E_{m1} and $E_{m2,}$ respectively, by:

$$E_{av}A = \int_A E\,\mathrm{d}A; \quad E_{m1}lA = \int_A Ey\,\mathrm{d}A; \quad E_{m2}I = \int_A Ey^2\,\mathrm{d}A \tag{2}$$

where A is the cross-sectional area of the undamaged layer, l is the thickness of the undamaged layer; and I is the moment of inertia ($I = \int_A y^2\,\mathrm{d}A$). The integrals in Equation (2) are evaluated numerically as the modulus E is dependent on the temperature distribution, which has been determined by the finite element analysis.

Due to the nonuniform modulus E the neutral axis of the column does not remain at the mid-surface during fire. The distance e of the neutral axis from the mid-surface axis x, is determined from:

$$e\int_A E(y)\mathrm{d}A = \int_A E(y)y\,\mathrm{d}A \tag{3}$$

which, by use of Equation (2) leads to:

$$e = \frac{E_{m1}l}{E_{av}}. \tag{4}$$

The thermal force along the longitudinal axis x is:

$$N_x^T = \int_A E(y)\alpha_l\Delta T(y)\mathrm{d}A \tag{5}$$

where the longitudinal thermal expansion coefficient α_l is assumed independent of temperature. Using Equation (2) and the temperature distribution results, the force given by Equation (5) can be evaluated numerically.

The thermal force developing due to the constraints at both ends of the column could cause buckling. However, in the case where one of the surfaces of the structure is exposed to fire, a bifurcation buckling is not observed as a result of a thermal moment that also develops. This moment (with respect to the neutral axis of the column) is:

$$M_Z^T = \int_A E(y)\alpha_l\Delta T(y)(y-e)\mathrm{d}A. \tag{6}$$

Therefore, it is necessary is to determine the response of the column under the influence of both N_x^T and M_Z^T, where the latter moment changes the character of the problem from bifurcation buckling to a bending problem.

We consider two cases: (a) the column constrained at the two ends which cannot move axially; (b) the column with axially unconstrained ends under a constant applied load P. In the former case, we assume that the external support force P that develops due to the boundaries is large enough to constrain the column, preventing axial displacements at both ends. Such situation is encountered in a long multi-span column with equally-spaced supports subject to a load independent of the axial coordinate. Then the boundaries of each span are prevented from axial displacements due to structural symmetry. In the present problem the axial force N_x does not vary with the axial position x. However, unlike the case of a uniformly heated column, the force P is smaller than N_x^T because of the expansion of the bent column caused by the thermal moment M_Z^T. In other words, the column bends away from its original straight configuration due to the thermal moment M_Z^T, which relieves some of the external support force at the immovable ends.

Notice that in the case of immovable ends P is a derived quantity, rather than a controlled quantity. In such case, the controlled quantity is the thermal loading due to the fire, while the response quantity is the transverse deflection of the column.

In the following subsection we illustrate three solutions. The next subsection represents the solution of the geometrically nonlinear problem followed by a the closed-form result obtained for the geometrically nonlinear formulation by the equivalent linearization method. Finally, in case of small deflections, typically limited to half-thickness of the depth of the noncharred cross-section, the linear solution is shown to be sufficiently accurate. The following solutions are applicable for both immovable as well as movable ends of the column.

Nonlinear Analysis

Let us denote by u_0 and w_0 the displacements along the axial x and transverse y directions at the neutral axis and by θ the rotation of the cross-section due to bending. The nonlinear strain at the neutral axis $y = e$, is:

$$\varepsilon_0 = u_{0,x} + \frac{1}{2}\theta^2. \tag{7}$$

In the following we account for the transverse shear following the procedure in Huang and Kardomateas [10]. In particular, we can set

$$\frac{\mathrm{d}w}{\mathrm{d}x} = \sin\left(\theta + \gamma_{eq}\right) \tag{8}$$

where γ_{eq} is the equivalent shear angle, i.e., a difference between the slope of the deflected column axis and the rotation θ of the cross-section due to bending.

It is reasonable to assume that the shear modulus, G, changes with temperature in the same manner as the elastic Young's modulus, E, implicitly neglecting the effect of fire on the Poisson ratio of an equivalent pseudo-isotropic E-glass/vinyl-ester material. Accordingly:

$$\begin{aligned}\frac{G}{G_0} &= 1 - a_1\left(\frac{T - T_0}{T_g - T_0}\right) + a_2\left(\frac{T - T_0}{T_g - T_0}\right)^2 - a_3\left(\frac{T - T_0}{T_g - T_0}\right)^3 \\ &= 1 - a_1\left(\frac{\Delta T}{\Delta T_g}\right) + a_2\left(\frac{\Delta T}{\Delta T_g}\right)^2 - a_3\left(\frac{\Delta T}{\Delta T_g}\right)^3.\end{aligned} \tag{9}$$

An effective shear modulus $\overline{G}$ is now defined based on the shear compliance as [10]:

$$\frac{l}{\overline{G}} = \int_{-l/2}^{l/2} \frac{\mathrm{d}y}{G(y)}. \tag{10}$$

The equivalent shear angle, γ_{eq}, is subsequently defined as:

$$\gamma_{eq} = \frac{\beta P \sin\theta}{\overline{G}\, A} \tag{11}$$

where β is the shear correction factor which accounts for the nonuniform distribution of shear stresses throughout the cross-section.

Then, the strain at an arbitrary point, $\overline{\varepsilon}(x, y)$, can be represented by

$$\overline{\varepsilon} = \varepsilon_0(x) - (y - e)\frac{\mathrm{d}\left(\theta + \gamma_{eq}\right)}{\mathrm{d}x}. \tag{12}$$

When the stress calculated using Equation (12) is integrated throughout the section, the resultant force should be equal to $-P + N_x^T$, i.e.:

$$\int_A E(y)\overline{\varepsilon}(x, y)\mathrm{d}A = -P + N_x^T. \tag{13}$$

Using Equations (7), (11), and (12), Equation (13) becomes:

$$E_{av}A\left(u_{0,x} + \frac{1}{2}\theta^2\right) + (E_{av}e - E_{m1}l)A\left(1 + \frac{\beta P\cos\theta}{\overline{G}A}\right)\theta_{,x} = N_x^T - P \tag{14}$$

The substitution of Equation (4) into Equation (14) yields:

$$u_{0,x} = \frac{N_x^T - P}{E_{av}A} - \frac{1}{2}\theta^2 \tag{15}$$

which we can integrate over the length of the column subject to the boundary conditions that the ends are restrained in the axial direction, i.e., $u_0(0) = 0$ and $u_0(L) = 0$ (case a). Performing the above-mentioned integration we obtain:

$$\left(N_x^T - P\right)\frac{L}{E_{av}A} - \frac{1}{2}\int_0^L \theta^2\,\mathrm{d}x = 0 \tag{16}$$

which is applicable for the entire loading range of the column. Equation (16) is a 'constraint equation' expressing the condition that the overall change in displacement between the end supports must be equal to zero because the ends of the column are immovable due to a support load P.

The effective bending rigidity $(EI)_{eq}$ of the column influenced by the nonuniform stiffness is defined by

$$(EI)_{eq} = \int_A E(y)(y - e)^2\mathrm{d}A. \tag{17}$$

Using Equations (2) and (4), Equation (17) becomes:

$$(EI)_{eq} = E_{m2}I - \frac{E_{m1}^2 l^2 A}{E_{av}}. \tag{18}$$

Next we modify the column equilibrium equation to account for the thermal loading including thermal force and moment, moderately large deflections and transverse shear. The moment accounting for the thermal effect on the material properties is given by:

$$M = -(EI)_{eq}\frac{d\theta}{dx} - M_z^T. \tag{19}$$

From equilibrium taking into account the compressive applied force, P, at both ends, the moment at an arbitrary position is given by:

$$M = Pw + M_0 \tag{20}$$

where M_0 is the moment at $x = 0$ that is equal to zero in case of simply supported ends.

Differentiating Equations (19) and (20) with respect to x and using Equations (8) and (11) with the additional assumption that the shear angle is small, so that $\sin\gamma_{eq} \approx \gamma_{eq}$ and $\cos\gamma_{eq} = 1$, results in:

$$(EI)_{eq}\frac{d^2\theta}{dx^2} + P\left(\frac{\beta P}{2A\overline{G}}\sin 2\theta + \sin\theta\right) + \frac{dM_z^T}{dx} = 0. \tag{21}$$

where the last term in the left side should be taken equal to zero since the heat flux and subsequently, the thermal moment are assumed independent of the axial coordinate.

The moment boundary conditions at the simply supported ends of the column are:

$$-(EI)_{eq}\frac{d\theta}{dx}(0) - M_z^T = 0; \quad -(EI)_{eq}\frac{d\theta}{dx}(L) - M_z^T = 0. \tag{22}$$

The solution process can now be outlined as follows. At each time instant, the temperature distribution and the thickness of the charred region are determined from the finite element analysis. Subsequently, the instantaneous values of the elastic and shear moduli are specified from Equations (1) and (9), respectively. The thermal force and thermal moment are found using Equations (5) and (6). In case (a), i.e., if the ends of the column are prevented from axial displacements, the application of the constraint condition (16) jointly with the equilibrium Equation (21) subject to boundary conditions (22) yields the rotation of the cross-section, i.e., θ, and the axial constraint force P. The rate of change of the axial displacements and the transverse deflection can now be determined from Equations (15) and (20), respectively.

In case (b), i.e., if the axial force applied to axially unconstrained column is prescribed, the integration of equation of equilibrium (21) subject to the boundary conditions (22) yields the rotation. The subsequent solution is identical to case (a). The methodology of the solution for both cases discussed above is illustrated in Figure 5.

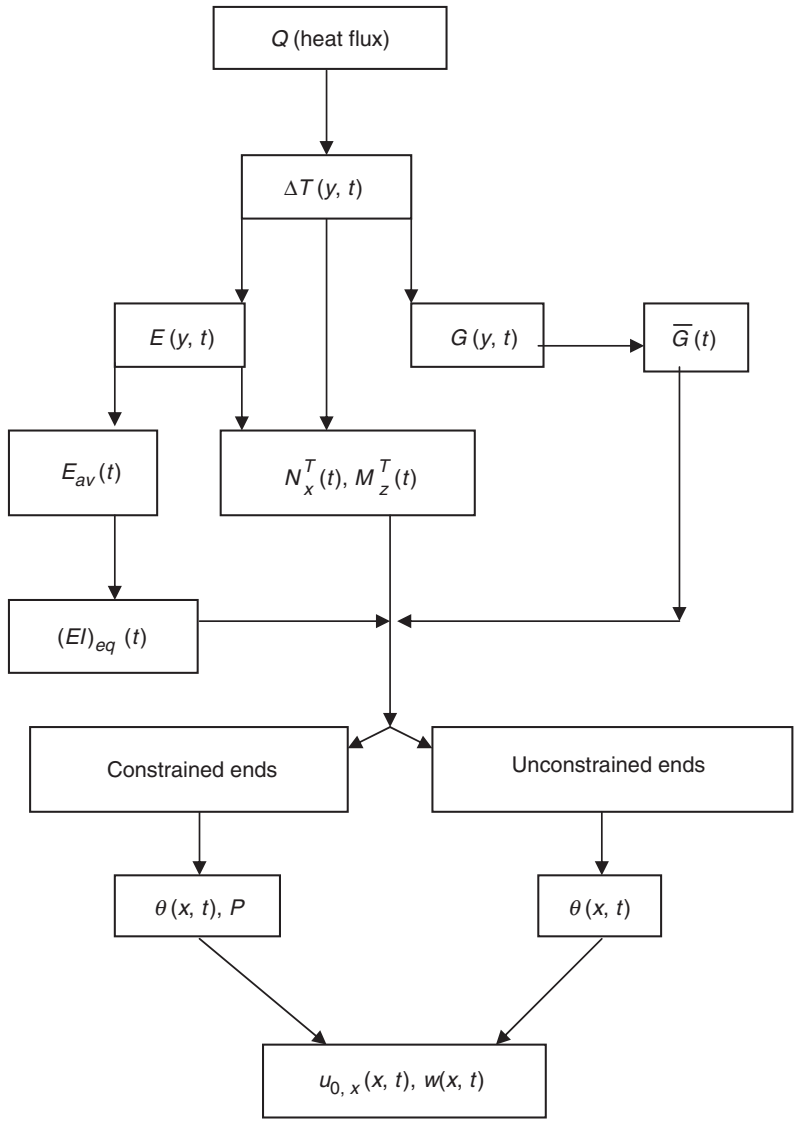

Figure 5. *Block-diagram with the sequence of the analysis of a geometrically nonlinear column subject to fire and compression.*

Closed-form Solution by Equivalent Linearization

Although the solution process explained above is straightforward it may be convenient to obtain a closed-form solution, even if it still requires a numerical analysis of the resulting equations. In this section, we illustrate such solution obtained through the linearization of the equation of equilibrium (21). The solution is applicable to case (b) where the ends are free to move axially, so that the axial force in the column is known. The analysis of case (a) conducted along the same lines is more complicated since it involves the necessity to linearize the 'constraint equation' (16).

We begin assuming that in a moderately nonlinear problem the number of terms in power series representing sine functions can be limited, so that:

$$\sin n\theta \approx n\,\theta - \frac{(n\theta)^3}{6} \quad (n = 1, 2). \tag{23}$$

Then, Equation (21) can be written as:

$$(EI)_{eq}\frac{\mathrm{d}^2\theta}{\mathrm{d}x^2} + \omega^2\theta - f\theta^3 = 0 \tag{24}$$

where:

$$\begin{aligned} \omega^2 &= P\left(\frac{\beta P}{A\overline{G}} + 1\right) \\ f &= \frac{P}{3}\left(\frac{2\beta P}{A\overline{G}} + \frac{1}{2}\right). \end{aligned} \tag{25}$$

According to the method of equivalent linearization (Panovko [11]), the nonlinear restoring force in Equation (24) is replaced with a linear counterpart yielding:

$$(EI)_{eq}\frac{\mathrm{d}^2\theta}{\mathrm{d}x^2} + \mu^2\theta = 0. \tag{26}$$

The value of constant μ^2 is found from the requirement that the overall squared error

$$r = \left(\omega^2\theta - f\theta^3\right) - \mu^2\theta \tag{27}$$

should be minimal over the range of variations of the function θ. In the present problem, θ varies from zero at the center of the column (assuming symmetric about the mid-span deformations as a result of the symmetry of the load and structure) to a still unknown maximum value at the end of the column. Another approach to the variation of θ could be to vary it from the minimum value at one end to the maximum value at the opposite end of the column (absolute values of these angles are equal), but it is easy to see that the results obtained by either method are identical. Accordingly, the minimization requirement implies:

$$\frac{\mathrm{d}}{\mathrm{d}\mu^2}\int_0^{\theta_{\max}} r^2\,\mathrm{d}\theta = 0. \tag{28}$$

Panovko [11] suggested that the 'impact' of the linearization increases at larger deviations from zero and accordingly, instead of the minimization of the overall squared error, it is more accurate to minimize the squared moment of this error:

$$\frac{\mathrm{d}}{\mathrm{d}\mu^2}\int_0^{\theta_{\max}} r^2\theta^2\,\mathrm{d}\theta = 0. \tag{29}$$

As was shown in the representative example in Ref. [11] equivalent linearization performed according to (29) yields a practically exact solution for a vibrating single degree of freedom system with cubic nonlinearity.

The result of the procedure described above can easily be shown:

$$\mu^2 = \omega^2 - \frac{5}{7} f \theta_{\max}^2. \tag{30}$$

The solution of Equation (26) is of course:

$$\theta = F_1 \sin \mu_1 x + F_2 \cos \mu_1 x, \quad \mu_1 = \frac{\mu}{\sqrt{(EI)_{eq}}}. \tag{31}$$

Now satisfying the boundary conditions (22) jointly with the requirement that $\theta(x=0) = \theta_{\max}$, we can specify constants F_1, $F_2$and the value of $\theta_{\max}$:

$$F_1 = -\frac{M_z^T}{\mu_1} \quad F_2 = \frac{M_z^T}{\mu_1} \frac{1 - \cos \mu_1 L}{\sin \mu_1 L}, \quad \theta_{\max} = F_2. \tag{32}$$

It is easy to show that $\theta_{\max} = \theta(0) = -\theta(L)$ and $\theta(L/2) = 0$.

The value of the maximum rotation corresponding to prescribed mechanical and thermal loads can be numerically determined from Equation (32). Subsequently, the analysis is conducted as is shown in the next section for the linear system with axially unconstrained ends.

Linear Thermoelastic Analysis

If deformations of the column remain limited, i.e., the problem is geometrically linear, differential Equation (21) can be linearized yielding a closed form solution. Taking into account the fact that the thermal moment M_z^T is independent of x, and using $\sin n\theta = n\theta$ ($n = 1, 2$), results in the linear equation:

$$(EI)_{eq} \frac{\mathrm{d}^2\theta}{\mathrm{d}x^2} + P\left(\frac{\beta P}{A\overline{G}} + 1\right)\theta = 0 \tag{33}$$

that can be solved subject to boundary conditions (22).

Introducing

$$\lambda^2 = \frac{P}{(EI)_{eq}} + \frac{\beta P^2}{(EI)_{eq} A\overline{G}} \tag{34}$$

the solution can be derived in the form:

$$\theta(x) = \frac{M_z^T}{\lambda (EI)_{eq}} \left[\frac{(1 - \cos \lambda L)}{\sin \lambda L} \cos \lambda L - \sin \lambda x \right]. \tag{35}$$

Note that the symmetry condition $\theta(L/2) = 0$ is satisfied by Equation (35).

Upon the linearization and using $\cos\theta \approx 1$, the constraint Equation (16) becomes

$$\left(N_x^T - P\right)\frac{L}{E_{av}A} - \frac{(M_z^T)^2}{2\left[(EI)_{eq}\lambda\right]^2}\frac{(1-\cos\lambda L)}{\sin\lambda L}\left(\frac{L}{\sin\lambda L} - \frac{1}{\lambda}\right) = 0. \tag{36}$$

The vertical deflection of the beam is obtained for the linear problem by using Equations (8) and (11) and integrating:

$$w(x) = \left(1 + \frac{\beta P}{\overline{G}A}\right)\int_0^x \theta(\xi)\,\mathrm{d}\xi. \tag{37}$$

Substituting Equation (35) into Equation (37) yields:

$$w(x) = \frac{M_z^T}{(EI)_{eq}\lambda^2}\left(1 + \frac{\beta P}{\overline{G}A}\right)\left[\frac{(1-\cos\lambda L)}{\sin\lambda L}\sin\lambda x + (\cos\lambda x - 1)\right]. \tag{38}$$

Note that from Equation (38) the deflections at the ends are zero (as they should be in a simply supported column), $w(0) = w(L) = 0$, and that the mid-point deflection, $w(L/2) = w_m$, is:

$$w_m = \frac{M_z^T}{(EI)_{eq}\lambda^2}\left(1 + \frac{\beta P}{\overline{G}A}\right)\left[\frac{1}{\cos(\lambda L/2)} - 1\right]. \tag{39}$$

The deflection given by Equation (39) becomes infinite for $\lambda L = \pi$ (the Euler load of the column).

Consider now case (a), i.e., the column with axially constrained ends. If the thermal loading is prescribed via the fire heat influx Q, then N_x^T and M_z^T can be determined, so that the only unknown in the right side of Equation (38) is P (or λ from Equation (34)). One can solve the transcendental Equation (36) for P, then use this value of the axial force in Equation (38) and thus obtain the relationship between the thermal loading Q and the transverse deflection, w. This relationship is obtained for constrained columns only and in this case, P, which is obtained from Equation (36), is the support reaction. On the other hand, if the 'constraint' condition of immovable supports is released (the second case where the ends are free to move axially), then P is the applied load and Equation (38) immediately provides the solution for transverse deflections. Numerical procedures for cases (a) and (b) described here are schematically depicted in Figure 6. Note that in the absence of the thermal moment M_z^T, the constraint Equation (36) reduces to $N_x^T = P$, i.e., the solution for a uniformly heated column.

NUMERICAL RESULTS AND DISCUSSION

Numerical results are presented for a composite pseudo-isotropic E-glass/vinyl-ester column, which is exposed to a heat flux $Q = 25\,\mathrm{kW/m^2}$. The length of the column is $L = 0.15\,\mathrm{m}$, its thickness is $H = 0.012\,\mathrm{m}$, and the width is $b = 0.025\,\mathrm{m}$. The original

quasi-isotropic E-glass/vinyl-ester has the following properties: $\alpha = 18.0 \times 10^6/^\circ\text{C}$; $E = 20.6\,\text{GPa}$; $G = 2.1\,\text{GPa}$ at room temperature which is $T_0 = 20^\circ\text{C}$.

Based on the thermal model/finite element analysis the temperature and charred layer thickness can be obtained as functions of time. In Figure 2, the temperature distribution throughout the thickness of the column exposed to a heat flux $Q = 25\,\text{kW/m}^2$ is shown for representative exposure times varying from 40 to 280 s. Since only the temperatures at the eight nodes are considered, the seventh order polynomial fit curves are obtained by the interpolation, which are subsequently used in the thermomechanical analysis. It is obvious that the temperature increases along with time t, eventually becoming more uniform throughout the thickness. In Figure 3, we show the charred layer thickness variation with time, where the residual resin content less than 80% is used as a criterion for the fully charred material. While the variation of residual resin content with time is continuous, the corresponding relationship in Figure 3 is not since the residual resin content (RRC) exceeding 80%, was treated as the undamaged material. Thus, the normalized charred layer thickness jumps at the time when the ratio of RRC becomes smaller than 80%.

The variation of the thickness of the charred layer was used in the quasi-static thermomechanical analysis that treated the column material by a two-layer approximation

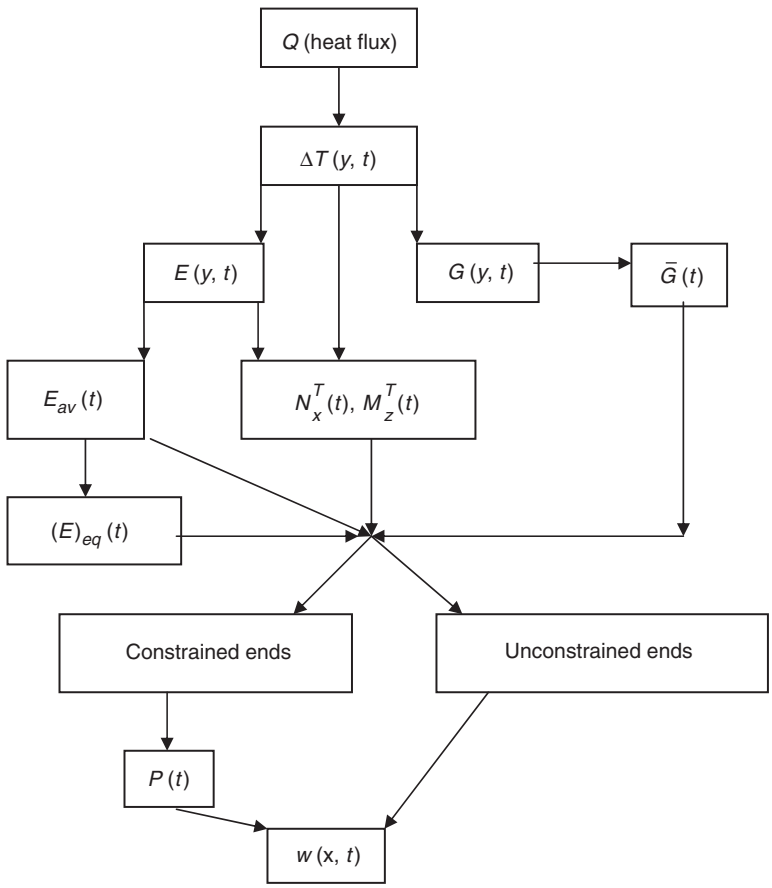

Figure 6. *Block-diagram with the sequence of the analysis of a geometrically linear column subject to fire and compression.*

where the undamaged layer was associated with the original material. The temperature distribution in the undamaged region obtained by the thermal/finite element model was used to analyze the thermal resultant force and moment, accounting for the variation of the material properties with temperature. The effect of temperature on the elastic modulus of E-glass/vinyl-ester composites is shown in Figure 4 referred to above. Moreover, since the experimental data are available only up to the glass transition temperature of the matrix, T_g, we assumed that beyond T_g, if the material is not charred yet, the elastic and shear modulus remain stable and do not decrease anymore.

With the quasi-static assumption, we analyze the thermomechanical response of the column at exposure times from $t = 0$ s until $t = 300$ s. The thermal moment developed in the column is shown as a function of the exposure time in Figure 7. The moment is not a continuous function of time since RRC is not continuous in the previous derivations based on a 80% breakpoint between the intact and fully charred material. The thermal moment variations reflect the temperature and material properties distributions within the column. At the beginning of the heat exposure, the resin material is rapidly decomposed due to high temperature and RRC varied with time continuously, but as $t < 60$ s, the RRC exceeds 80% throughout the entire column, so that we neglect the presence of a charred material. The thermal moment increases from the beginning of the heat exposure $t = 0$ s until $t = 60$ s, which is due to the continuous temperature variation in the column. Within the exposure time interval between $t = 60$ s and $t = 140$ s, a part of material (1/7 of the entire thickness of the column) is charred according to Figure 3 and the properties of the charred material are neglected. Accordingly, the absolute value of the thermal moment is reduced during this time interval as a result of the decreasing effective thickness of the column and the corresponding variation of temperature. With the further increasing exposure time, more material is charred and the thermal moment decreases accordingly.

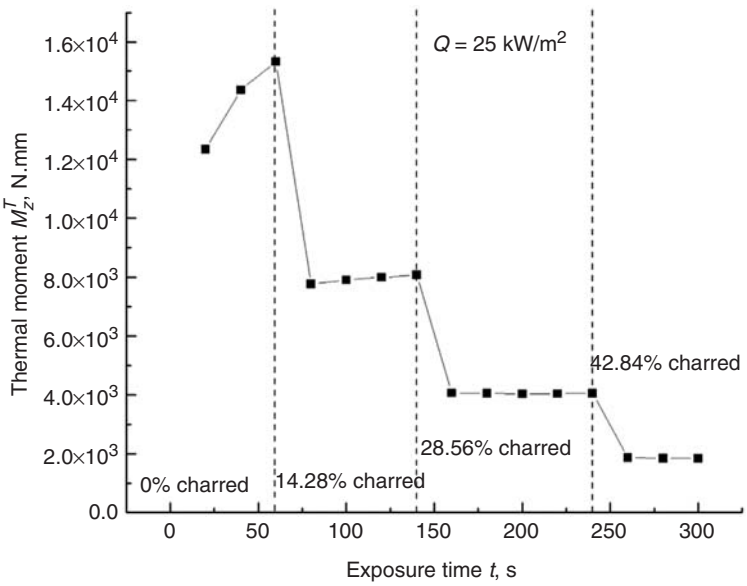

Figure 7. *Thermal moment developed in the column vs. exposure time. The moment is not a continuous function, since the residual resin content does not account for a continuous variation with exposure time.*

The axial constraint stress σ_{xx} in a simply supported axially constrained column (case a) subject to the heat flux $Q = 25\,\text{kW/m}^2$ is shown as a function of time in Figure 8. The stress increases with time at $t < 140\,\text{s}$, but the trend is reversed and σ_{xx} decreases with exposure time $t > 140\,\text{s}$; the second order polynomial curve was obtained to approximately fit the variation trend. We can analyze the variation of the axial constraint by dividing the exposure time into four zones, the thickness of charred material being constant within each zone (these zones are reflected in Figure 3). It is observed that the variation of the constraint stress is nonlinear in each zone, which is due to the material properties that nonlinearly decrease with the exposure time. There exists a peak value of the axial constraint stress at exposure time $t = 140\,\text{s}$. The fact that σ_{xx} decreases beyond this instant indicates that at a certain level of deformation the structure starts to 'pull' from the ends rather than 'push' against the ends.

The mid-point deflection w_m normalized by the original thickness of the column is shown in Figure 9. The variation of the mid-point deflection with time is not smooth; however, the linear curve can adequately fit it, except for the initial time interval. It can be observed that in general, the mid-point deflection of the column increases with the exposure time. The direction of the mid-point is always positive, implying that the column bends toward the heat source under the constrained boundary conditions.

Experimental studies on fiber-reinforced vinyl-ester (Derakane 510A) columns with constrained end cross-section were reported elsewhere (see for example, Ref. [5]). In general, the results of these studies confirmed the theoretical predictions of the present article. For example, a positive deflection was observed in the tests for the column exposed to the heat flux $Q = 25\,\text{kW/m}^2$ under the constant compressive axial load P, corresponding to a stress of 10.5 MPa (based on the thickness of the original section). At the same time, it was noted that in the case of fire of low intensity, the decomposition of resin does not occur.

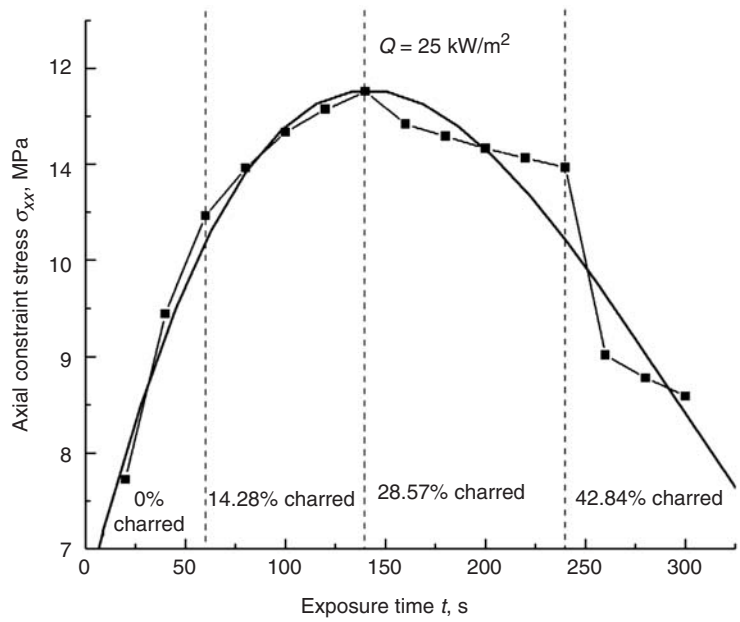

Figure 8. *The axial constraint stress σ_{xx} vs. exposure time t. A second order polynomial curve was obtained to fit the variation trend.*

For example, the failure mode of the column subject to the above-mentioned loading is shown in Figure 10 [5]. In this case the failure took place prior to the resin decomposition as a result of a combination of the thermally-induced properties deterioration, thermal bending, and consequent eccentricity of loading. As is obvious from Figure 10, the final phase of the response is characterized by massive delaminations. This would justify the use of a nonlinear finite element analysis to trace the final phase of the response. However, the degree of damage accumulated prior to such catastrophic event makes the column

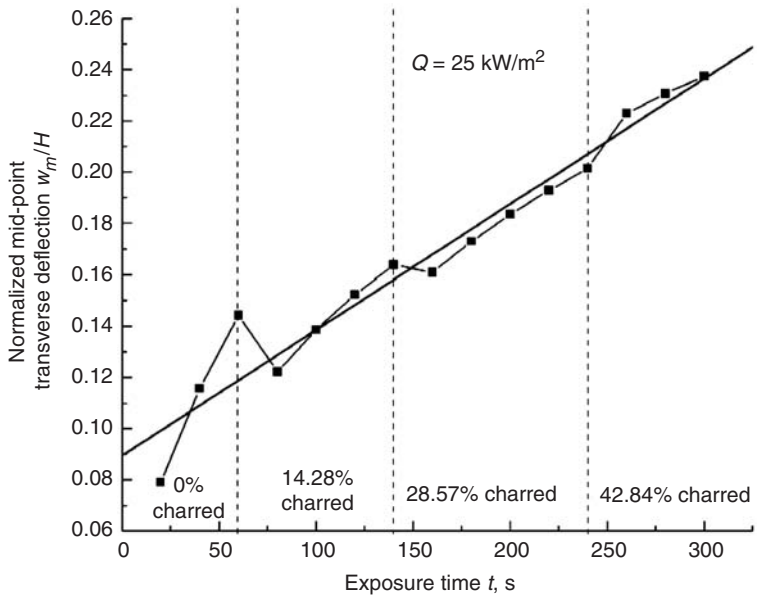

Figure 9. *The normalized mid-point transverse deflection vs. exposure time for the constrained column (case (a)) under the heat flux due to fire, $Q = 25\,kW/m^2$.*

Figure 10. *The failed fiberglass reinforced composite column exposed to the fire heat flux $Q = 25\,kW/m^2$ under the constant axial compressive load, P, corresponding to a stress of 10.5 MPa (the stress is calculated based on the original section geometry).*

unusable, i.e., the analysis of the initial damage onset available using the present solution should be sufficient for most applications.

CONCLUSIONS

The solution for the response of a composite column exposed to a heat flux due to fire and an axial compressive load is considered. Two boundary conditions analyzed in the article include the cases where the column is axially restrained (immovable ends) and where the ends are free to move axially (no axial restrain). The temperature and charred material thickness distributions are obtained by the thermal/finite element method of Gibson analyzing the heat response problem for the polymer composite material. Subsequently, this temperature and charred thickness profile are employed in conjunction with the temperature-dependent moduli of the composite material to analyze the thermomechanical response. The solution is obtained assuming that the mechanical properties of the charred layer are negligible. Both geometric nonlinearity as well as shear deformability can be included in the analysis.

The following conclusions follow from the analysis:

1. The thermal moment induced in the column during fire decreases with the exposure time due to the resin material decomposition and the gradual development of the charred layer.
2. The variation of the axial constraint stress in the constrained column with the exposure time is nonlinear; there exists a peak value followed with a decrease of the constraint stress. This phenomenon is related to the variation of the char thickness, membrane stresses produced as a result of increasing lateral deflections, and the non-linear temperature and material properties distributions in the undamaged composite.
3. The deflection of the constrained column increases with the heat exposure time (approximately in a linear fashion). The bending deformation occurs toward the heat source, which is consistent with the experimental observation for the similar column.
4. The thermal bending moment is unavoidable in the structures subject to fire on one surface. This moment causes out-of-plane transverse deflection from the onset of heat exposure. Therefore, the problem of bifurcation buckling does not exist in structures undergoing fire; instead such structures experience thermally-induced bending (it could be shown that an exception is found in clamped structures subject to fire that produces a uniform heat flux over the entire exposed surface).

ACKNOWLEDGMENT

The financial support of the Office of Naval Research, Grant N00014-03-1-0189, is gratefully acknowledged.

REFERENCES

1. Gibson, A.G., Wu, Y.S., Chandler, H.W., Wilcox, J.A.D. and Bettess, P. (1995). A Model for the Thermal Performance of Thick Composite Laminates in Hydrocarbon Fires, In Composite Materials in the Petroleum Industry, *Revue de l'Institute Francais du Petrole*, **50**: 69–74.

2. Sorathia, U., Rollhauser, C.M. and Hughes, W.A. (1992). Improved Fire Safety of Composites for Naval Applications, *Fire Mater.*, **16**: 119–125.
3. Gibson, A.G. and Hume, J. (1995). Fire Performance of Composite Panels for Large Marine Structures, *Plast. Rubber Compos. Process. Appl.*, **23**: 175–183.
4. Mouritz, A.P. and Gardiner, C.P. (2002). Compression Properties of Fire-Damaged Polymer Sandwich Composites, *Composites Part A*, **33**: 609–620.
5. Liu, L., Kardomateas, G.A., Birman, V., Holmes, J.W. and Simitses, G.J. (2006). Thermal Buckling of a Heat-Exposed, Axially Restrained Composite Column, *Composites Part A*, **37**: 972–980.
6. Henderson, J.B., Wiebelt, J.A. and Tant, M.R. (1985). A Model for the Thermal Response of Polymer Composite Materials with Experimental Verification, *Journal of Composite Materials*, **19**: 579–595.
7. Looyeh, M.R.E., Bettess, P. and Gibson, A.G. (1997). A One-dimensional Finite Element Simulation for the Fire-performance of GRP Panels for Offshore Structures, *International Journal of Numerical Methods for Heat and Fluid Flow*, **7**(6): 609–625.
8. Gibson, A.G., Wright, P.N.H., Wu, S.Y., Mouritz, A.P. et al. (2003). Modeling Residual Mechanical Properties of Polymer Composites after Fire, *Plastic, Rubber and Composites*, **32**(2): 81–90.
9. Kulkarni, A.P. and Gibson, R.F. (2003). Nondestructive Characterization of Effects of Temperature and Moisture on Elastic Moduli of Vinyl ester Resin and E-glass/vinylester Composite. In: *Proceedings of the American Society of Composites 18th Annual Technical Conference*. Florida.
10. Huang, H. and Kardomateas, G.A. (2002). Buckling and Initial Postbuckling Behavior of Sandwich Beams Including Transverse Shear, *AIAA Journal*, **40**(11): 2331–2335.
11. Panovko, Ya.G. (1976). *Foundations of Applied Theory of Vibrations and Impact*, **3rd edn**, Mashinostroenie Publishers, Leningrad (in Russian).